

The disruption of the Magellanic Stream

J. Bland-Hawthorn

School of Physics, University of Sydney, NSW 2006, Australia
email: jbh@physics.usyd.edu.au

Abstract. We present evidence that the accretion of warm gas onto the Galaxy today is at least as important as cold gas accretion. For more than a decade, the source of the bright H α emission (up to 750 mR \dagger) along the Magellanic Stream has remained a mystery. We present a hydrodynamical model that explains the known properties of the H α emission and provides new insights on the lifetime of the Stream clouds. The upstream clouds are gradually disrupted due to their interaction with the hot halo gas. The clouds that follow plough into gas ablated from the upstream clouds, leading to shock ionisation at the leading edges of the downstream clouds. Since the following clouds also experience ablation, and weaker H α (100–200 mR) is quite extensive, a disruptive cascade must be operating along much of the Stream. In order to light up much of the Stream as observed, it must have a small angle of attack ($\approx 20^\circ$) to the halo, and this may already find support in new HI observations. Another prediction is that the Balmer ratio (H α /H β) will be substantially enhanced due to the slow shock; this will soon be tested by upcoming WHAM observations in Chile. We find that the clouds are evolving on timescales of 100–200 Myr, such that the Stream must be replenished by the Magellanic Clouds at a fairly constant rate ($\gtrsim 0.1 M_\odot \text{ yr}^{-1}$). The ablated material falls onto the Galaxy as a warm drizzle; diffuse ionized gas at 10^4 K is an important constituent of galactic accretion. The observed H α emission provides a new constraint on the rate of disruption of the Stream and, consequently, the infall rate of metal-poor gas onto the Galaxy. When the ionized component of the infalling gas is accounted for, the rate of gas accretion is $\gtrsim 0.4 M_\odot \text{ yr}^{-1}$, roughly twice the rate deduced from HI observations alone.

Keywords. hydrodynamics, instabilities, shock waves, galaxies: evolution, galaxies: interactions, Magellanic Clouds

1. Introduction

It is now well established that the observed baryons over the electromagnetic spectrum account for only a fraction of the expected baryon content in Lambda Cold Dark Matter cosmology. This is true on scales of galaxies, in particular, within the Galaxy where easily observable phases have been studied in great detail over many years. The expected baryon fraction ($\Omega_B/\Omega_{DM} \approx 0.17$) of the dark halo mass ($1.4 \times 10^{12} M_\odot$; Smith *et al.* 2007) leads to an expected baryon mass of $2.4 \times 10^{11} M_\odot$ but a detailed inventory reveals only a quarter of this mass (Flynn *et al.* 2006). Moreover, the build-up of stars in the Galaxy requires an accretion rate of $1\text{--}3 M_\odot \text{ yr}^{-1}$ (Williams & McKee 1997; Binney *et al.* 2000), at least a factor of 4 larger than what can be accounted for from direct observation. The derived baryon mass may be a lower bound if the upward correction in the LMC-SMC orbit motion reflects a larger halo mass (Kallivayalil *et al.* 2006; Piatek *et al.* 2008; cf. Wilkinson & Evans 1999). Taken together, these statements suggest that most of the baryons on scales of galaxies have yet to be observed.

\dagger 1 Rayleigh (R) = $10^6/4\pi$ photons $\text{cm}^{-2} \text{ s}^{-1} \text{ sr}^{-1}$, equivalent to 5.7×10^{-18} erg $\text{cm}^{-2} \text{ s}^{-1} \text{ arcsec}^{-2}$ at H α .

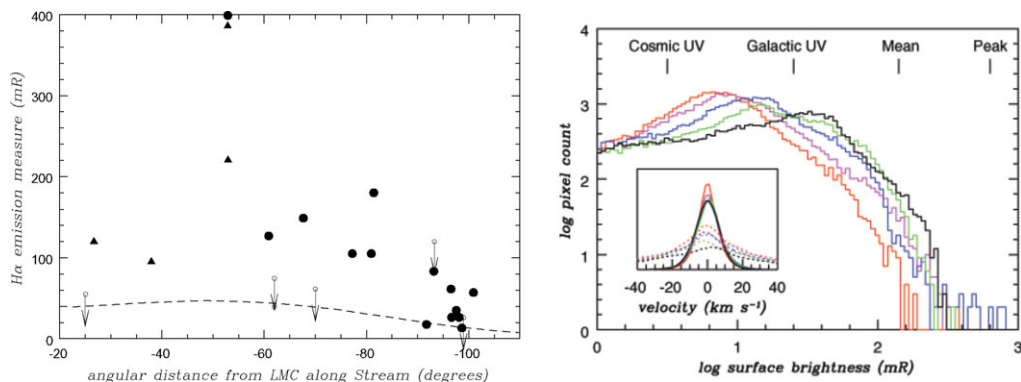


Figure 1. **Left:** $H\alpha$ measurements and upper limits along the Stream. The filled circles are from the WHAM survey by Madsen *et al.* (2002); the filled triangles are from the TAURUS survey by Putman *et al.* (2003). The dashed line model is the $H\alpha$ emission measure induced by the ionizing intensity of the Galactic disk (Bland-Hawthorn & Maloney 1999, 2002); this fails to match the Stream's $H\alpha$ surface brightness by at least a factor of 3. **Right:** the evolving distribution of projected $H\alpha$ emission as the shock cascade progresses. The timesteps are 70 (red), 120 (magenta), 170 (blue), 220 (green) and 270 Myr (black). The extreme emission measures increase with time and reach the observed mean values after 120 Myr; this trend in brightness arises because denser material is ablated as the cascade evolves. The mean and peak emission measures along the Stream are indicated, along with the approximate contributions from the cosmic and Galactic UV backgrounds. **Inset:** The evolving $H\alpha$ line width as the shock cascade progresses; the velocity scale is with respect to the reference frame of the initial H I gas. The solid lines are flux-weighted line profiles; the dashed lines are volume-weighted profiles that reveal more extreme kinematics at the lowest densities.

So how do galaxies accrete their gas? Is the infalling gas confined by dark matter? Does the gas arrive cold, warm or hot? Does the gas rain out of the halo onto the disk or is it forced out by the strong disk-halo interaction? These issues have never been resolved, either through observation or through numerical simulation. HI observations of the nearby universe suggest that galaxy mergers and collisions are an important aspect of this process, but tidal interactions do not guarantee that the gas settles to one or other galaxy. The most spectacular interaction phenomenon is the Magellanic HI Stream that trails from the LMC-SMC system (10:1 mass ratio) in orbit about the Galaxy. Since its discovery in the 1970s, there have been repeated attempts to explain the Stream in terms of tidal and/or viscous forces (q.v. Mastrogiuseppe *et al.* 2005; Connors *et al.* 2006). Indeed, the Stream has become a benchmark against which to judge the credibility of N-body+gas codes in explaining gas processes in galaxies. A fully consistent model of the Stream continues to elude even the most sophisticated codes.

Here, we demonstrate that $H\alpha$ detections along the Stream (Fig. 1) are providing new insights on the present state and evolution of the HI gas. At a distance of $D \approx 55$ kpc, the expected $H\alpha$ signal excited by the cosmic and Galactic UV backgrounds are about 3 mR and 25 mR respectively (Bland-Hawthorn & Maloney 1999, 2002), significantly lower than the mean signal of 100–200 mR, and much lower than the few bright detections in the range 400–750 mR (Weiner *et al.* 2002). This signal cannot have a stellar origin since repeated attempts to detect stars along the Stream have failed.

Some of the Stream clouds exhibit compression fronts and head-tail morphologies (Brüns *et al.* 2005) and this is suggestive of confinement by a tenuous external medium. But the cloud:halo density ratio ($\eta = \rho_c / \rho_h$) necessary for confinement can be orders of magnitude *larger* than that required to achieve shock-induced $H\alpha$ emission (e.g. Quilis & Moore 2001). Indeed, the best estimates of the halo density at the distance of the Stream

($\rho_{\text{h}} \sim 10^{-4} \text{ cm}^{-3}$; Bregman 2007) are far too tenuous to induce strong $\text{H}\alpha$ emission at a cloud face. It is therefore surprising to discover that the brightest $\text{H}\alpha$ detections lie at the leading edges of H I clouds (Weiner *et al.* 2002) and thus appear to indicate that shock processes are somehow involved.

We summarize a model, first presented in Bland-Hawthorn *et al.* (2007), that goes a long way towards explaining the $\text{H}\alpha$ mystery. The basic premise is that a tenuous external medium not only confines clouds, but also disrupts them with the passage of time. The growth time for Kelvin-Helmholtz (KH) instabilities is given by $\tau_{\text{KH}} \approx \lambda \eta^{0.5} / v_{\text{h}}$ where λ is the wavelength of the growing mode, and v_{h} is the apparent speed of the halo medium ($v_{\text{h}} \approx 350 \text{ km s}^{-1}$; see §2). At the distance of the Stream, the expected timescale for KH instabilities is less than for Rayleigh-Taylor (RT) instabilities. For cloud sizes of order a few kiloparsecs and $\xi \approx 10^4$, the KH timescale can be much less than an orbital time ($\tau_{\text{MS}} \approx 2\pi D / v_{\text{h}} \approx 1 \text{ Gyr}$). Once an upstream cloud becomes disrupted, the fragments are slowed with respect to the LMC-SMC orbital speed and are subsequently ploughed into by the following clouds.

2. A new hydrodynamical model

We investigate the dynamics of the Magellanic Stream with two independent hydrodynamics codes, FYRIS and RAMSES, that solve the equations of gas dynamics with adaptive mesh refinement. The results shown here are from the FYRIS code because it includes non-equilibrium ionization, but we get comparable gas evolution from either code†.

The brightest emission is found along the leading edges of clouds MS II, III and IV with values as high as 750 mR for MS II. The $\text{H}\alpha$ line emission is clearly resolved at 20–30 km s^{-1} FWHM, and shares the same radial velocity as the H I emission within the measurement errors (Weiner *et al.* 2002; G. Madsen 2007, personal communication). This provides an important constraint on the physical processes involved in exciting the Balmer emission.

In order to explain the $\text{H}\alpha$ detections along the Stream, we concentrate our efforts on the disruption of the clouds labelled MS I–IV (Brüns *et al.* 2005). The Stream is trailing the LMC-SMC system in a counter-clockwise, near-polar orbit as viewed from the Sun. The gas appears to extend from the LMC dislodged through tidal disruption although some contribution from drag must also be operating (Moore & Davis 1994). Recently, the Hubble Space Telescope has determined an orbital velocity of $378 \pm 18 \text{ km s}^{-1}$ for the LMC. While this is higher than earlier claims, the result has been confirmed by independent researchers (Piatek *et al.* 2008). Besla *et al.* (2007) conclude that the origin of the Stream may no longer be adequately explained with existing numerical models. The Stream velocity along its orbit must be comparable to the motion of the LMC; we adopt a value of $v_{\text{MS}} \approx 350 \text{ km s}^{-1}$.

Here we employ a 3D Cartesian grid with dimensions $18 \times 9 \times 9 \text{ kpc}$ [$(x, y, z) = (432, 216, 216)$ cells] to model a section of the Stream where x is directed along the Stream arc and the z axis points towards the observer. The grid is initially filled with two gas components. The first is a hot thin medium representing the halo corona.

Embedded in the hot halo is (initially) cold H I material with a total H I mass of $3 \times 10^7 M_{\odot}$. The cold gas has a fractal distribution and is initially confined to a cylinder with a diameter of 4 kpc and length 18 kpc; the mean volume and column densities are 0.02 cm^{-3} and $2 \times 10^{19} \text{ cm}^{-2}$ respectively. The 3D spatial power spectrum ($P(k) \propto k^{-5/3}$)

† Further details on the codes and comparative simulations are provided at <http://www.aao.gov.au/astro/MS>.

describes a Kolmogorov turbulent medium with a minimum wavenumber k corresponding to a spatial scale of 2.25 kpc, comparable to the size of observed clouds along the Stream.

We consider the hot corona to be an isothermal gas in hydrostatic equilibrium with the gravitational potential, $\phi(R, z)$, where R is the Galactocentric radius and z is the vertical scale height. We adopt a total potential of the form $\phi = \phi_d + \phi_h$ for the disk and halo respectively; for our calculations at the Solar Circle, we ignore the Galactic bulge. The galaxy potential is defined by

$$\phi_d(R, z) = -c_d v_{\text{circ}}^2 / \left(R^2 + \left(a_d + \sqrt{z^2 + b_d^2} \right)^2 \right)^{0.5} \tag{2.1}$$

$$\phi_h(R, z) = c_h v_{\text{circ}}^2 \ln((\psi - 1)/(\psi + 1)) \tag{2.2}$$

and $\psi = (1 + (a_h^2 + R^2 + z^2)/r_h^2)^{0.5}$. The scaling constants are $(a_d, b_d, c_d) = (6.5, 0.26, 8.9)$ kpc and $(a_h, r_h) = (12, 210)$ kpc with $c_h = 0.33$ (e.g., Miyamoto & Nagai 1975; Wolfire *et al.* 1995). The circular velocity $v_{\text{circ}} \approx 220 \text{ km s}^{-1}$ is now well established through wide-field stellar surveys (Smith *et al.* 2007).

We determine the vertical acceleration at the Solar Circle using $g = -\partial\phi(R_o, z)/\partial z$ with $R_o = 8$ kpc. The hydrostatic halo pressure follows from

$$\frac{\partial\phi}{\partial z} = -\frac{1}{\rho_h} \frac{\partial P}{\partial z} \tag{2.3}$$

After Ferrara & Field (1994), we adopt a solution of the form $P_h(z) = P_o \exp((\phi(R_o, z) - \phi(R_o, 0))/\sigma_h^2)$ where σ_h is the isothermal sound speed of the hot corona. To arrive at P_o , we adopt a coronal halo density of $n_{e,h} = 10^{-4} \text{ cm}^{-3}$ at the Stream distance (55 kpc) in order to explain the Magellanic Stream H α emission (Bland-Hawthorn *et al.* 2007), although this is uncertain to a factor of a few. We choose $T_h = 2 \times 10^6 \text{ K}$ to ensure that O VI is not seen in the diffuse corona consistent with observation (Sembach *et al.* 2003); this is consistent with a rigorously isothermal halo for the Galaxy.

A key parameter of the models is the ratio of the cloud to halo pressure, $\xi = P_c/P_h$. If the cloud is to survive the impact of the hot halo, then $\xi \gtrsim 1$. A shocked cloud is destroyed in about the time it takes for the internal cloud shock to cross the cloud, during which time the cool material mixes and ablates into the gas streaming past. Only massive clouds with dense cores can survive the powerful shocks. An approximate lifetime \dagger for a spherical cloud of diameter d_c is

$$\tau_c = 60(d_c/2 \text{ kpc})(v_h/350 \text{ km s}^{-1})^{-1}(\eta/100)^{0.5} \text{ Myr.} \tag{2.4}$$

For η in the range of 100–1000, this corresponds to 60–180 Myr for individual clouds. With a view to explaining the H α observations, we focus our simulations on the lower end of this range.

For low η , the density of the hot medium is $n_h = 2 \times 10^{-4} \text{ cm}^{-3}$. The simulations are undertaken in the frame of the cold H I clouds, so the halo gas is given an initial transverse velocity of 350 km s^{-1} . The observations reveal that the mean H α emission has a slow trend along the Stream which requires the Stream to move through the halo at a small angle of attack (20°) in the plane of the sky in order to explain the more distribution emission. Independent evidence for this appears to come from a wake of low column clouds along the Stream (Westmeier & Koribalski 2008). Thus, the velocity of the hot gas as seen by the Stream is $(v_x, v_y) = (-330, -141) \text{ km s}^{-1}$. The adiabatic sound

\dagger Here we correct a typo in equation (1) of Bland-Hawthorn *et al.* (2007).

speed of the halo gas is 200 km s^{-1} , such that the drift velocity is mildly supersonic (transsonic), with a Mach number of 1.75.

A unique feature of the FYRIS simulations is that they include non-equilibrium cooling through time-dependent ionisation calculations (cf. Rosen & Smith 2004). When shocks occur within the inviscid fluid, the jump shock conditions are solved across the discontinuity. This allows us to calculate the Balmer emission produced in shocks and additionally from turbulent mixing along the Stream (e.g., Slavin *et al.* 1993). We adopt a conservative value for the gas metallicity of $[\text{Fe}/\text{H}] = -1.0$ (cf. Gibson *et al.* 2000); a higher value accentuates the cooling and results in denser gas, and therefore stronger $\text{H}\alpha$ emission along the Stream.

2.1. Results

The main results of the simulations are presented elsewhere (Bland-Hawthorn *et al.* 2007: see animations at <http://www.ao.gov.au/astro/MS>). In our model, the fractal Stream experiences a “hot wind” moving in the opposite direction. The sides of the Stream clouds are subject to gas ablation via KH instabilities due to the reduced pressure (Bernoulli’s theorem). The ablated gas is slowed dramatically by the hot wind and is transported behind the cloud. As higher order modes grow, the fundamental mode associated with the cloud size will eventually fragment it. The ablated gas now plays the role of a “cool wind” that is swept up by the pursuing clouds leading to shock ionization and ablation of the downstream clouds. The newly ablated material continues the trend along the length of the Stream. The pursuing gas cloud transfers momentum to the ablated upstream gas and accelerates it; this results in Rayleigh-Taylor (RT) instabilities, especially at the stagnation point in the front of the cloud. We rapidly approach a nonlinear regime where the KH and RT instabilities become strongly entangled, and the internal motions become highly turbulent. The simulations track the progression of the shock fronts as they propagate into the cloudlets.

Bland-Hawthorn *et al.* (2007, Fig. 2) show the predicted conversion of neutral to ionized hydrogen due largely to cascading shocks along the Stream. The drift of the peak to higher columns is due to the shocks eroding away the outer layers, thereby progressing into increasingly dense cloud cores. The ablated gas drives a shock into the H I material with a shock speed of v_s measured in the cloud frame. At the shock interface, once ram-pressure equilibrium is reached, we find $v_s \approx v_h \eta^{-0.5}$. In order to produce significant $\text{H}\alpha$ emission, $v_s \gtrsim 35 \text{ km s}^{-1}$ such that $\eta \lesssim 100$. In Fig. 1, we see the predicted steady rise in $\text{H}\alpha$ emission along the Stream, reaching 100–200 mR after 120 Myr, and the most extreme observed values after 170 Myr. The power-law decline to bright emission measures is a direct consequence of the shock cascade. The shock-induced ionization rate is $1.5 \times 10^{47} \text{ phot s}^{-1} \text{ kpc}^{-1}$. The predicted luminosity-weighted line widths of 20 km s^{-1} FWHM are consistent with the $\text{H}\alpha$ kinematics. In our models, much the $\text{H}\alpha$ lies at the leading edges of clouds, although there are occasional cloudlets where ionized gas dominates over the neutral column. Some of the brightest emission peaks appear to be due to limb brightening, while others arise from chance alignments.

2.2. Discussion

We have seen that the brightest $\text{H}\alpha$ emission along the Stream can be understood in terms of shock ionization and heating in a transsonic (low Mach number) flow. For the first time, the Balmer emission (and associated emission lines) provides diagnostic information at any position along the Stream that is independent of the H I observations. Slow Balmer-dominated shocks of this kind (e.g., Chevalier & Raymond 1978) produce partially ionized media where a significant fraction of the $\text{H}\alpha$ emission is due to collisional excitation. This

can lead to Balmer decrements ($H\alpha/H\beta$ ratio) in excess of 4, i.e. significantly enhanced over the pure recombination ratio of about 3, that will be fairly straightforward to verify in the brightest regions of the Stream.

The shock models predict a range of low-ionization emission lines (e.g., O I, S II), some of which will be detectable even though suppressed by the low gas-phase metallicity. There are likely to be EUV absorption-line diagnostics through the shock interfaces revealing more extreme kinematics, but these detections (e.g., O VI) are only possible towards fortuitous background sources (Sembach *et al.* 2001; Bregman 2007). The predicted EUV/X-ray emissivity from the post-shock regions is much too low to be detected in emission.

The characteristic timescale for large changes is roughly 100–200 Myr, and so the Stream needs to be replenished by the outer disk of the LMC at a fairly constant rate (e.g., Mastropietro *et al.* 2005). The timescale can be extended with larger η values (equation (2.4)), but at the expense of substantially diminished $H\alpha$ surface brightness. In this respect, we consider η to be fairly well bounded by observation and theory.

What happens to the gas shedded from the dense clouds? Much of the diffuse gas will become mixed with the hot halo gas suggesting a warm accretion towards the inner Galactic halo. If most of the Stream gas enters the Galaxy via this process, the derived gas accretion rate is $\sim 0.4 M_{\odot} \text{ yr}^{-1}$. The higher value compared to H I (e.g., Peek *et al.* 2008) is due to the gas already shredded, not seen by radio telescopes now. In our model, the HVCs observed today are unlikely to have been dislodged from the Stream by the process described here. These may have come from an earlier stage of the LMC-SMC interaction with the outer disk of the Galaxy.

The “shock cascade” interpretation for the Stream clears up a nagging uncertainty about the $H\alpha$ distance scale for high-velocity clouds. Bland-Hawthorn *et al.* (1998) first showed that distance limits to HVCs can be determined from their observed $H\alpha$ strength due to ionization by the Galactic radiation field, now confirmed by clouds with reliable distance brackets from the stellar absorption line technique (Putman *et al.* 2003; Lockman *et al.* 2008; Wakker *et al.* 2007). HVCs have smaller kinetic energies compared to the Stream clouds, and their interactions with the halo gas are not expected to produce significant shock-induced or mixing layer $H\alpha$ emission, thereby supporting the use of $H\alpha$ as a crude distance indicator.

If we are to arrive at a satisfactory understanding of the Stream interaction with the halo, future deep $H\alpha$ surveys will be essential. It is plausible that current $H\alpha$ observations are still missing a substantial amount of gas, in contrast to the deepest H I observations. We can compare the particle column density inferred from H I and $H\alpha$ imaging surveys. The limiting H I column density is about $N_{\text{H}} \approx \langle n_{\text{H}} \rangle L \approx 10^{18} \text{ cm}^{-2}$ where $\langle n_{\text{H}} \rangle$ is the mean atomic hydrogen density, and L is the depth through the slab. By comparison, the $H\alpha$ surface brightness can be expressed as an equivalent emission measure, $E_{\text{m}} \approx \langle n_{\text{e}}^2 \rangle L \approx \langle n_{\text{e}} \rangle N_{\text{e}}$. Here n_{e} and N_{e} are the local and column electron density. The limiting value of E_{m} in $H\alpha$ imaging is about 100 mR, and therefore $N_{\text{e}} \approx 10^{18} / \langle n_{\text{e}} \rangle \text{ cm}^{-2}$. Whether the ionized and neutral gas are mixed or distinct, we can hide a lot more ionized gas below the imaging threshold for a fixed L , particularly if the gas is at low density ($\langle n_{\text{e}} \rangle \ll 0.1 \text{ cm}^{-3}$). A small or variable volume filling factor can complicate this picture but, in general, the ionized gas still wins out because of ionization of low density H I by the cosmic UV background (Maloney 1993). In summary, even within the constraints of the cosmic microwave background (see Maloney & Bland-Hawthorn 1999), a substantial fraction of the gas can be missed if it occupies a large volume in the form of a low density plasma.

References

- Besla, G., Kallivayalil, N., Hernquist, L., *et al.* 2007, *ApJ*, 668, 949
- Binney, J., Dehnen, W., & Bertelli, G. 2000, *MNRAS*, 318, 658
- Bland-Hawthorn, J., Veilleux, S., Cecil, G. N., Putman, M. E., Gibson, B. K., & Maloney, P. R. 1998, *MNRAS*, 299, 611
- Bland-Hawthorn, J. & Maloney, P. R. 1999, *ApJ*, 510, L33
- Bland-Hawthorn, J. & Maloney, P. R. 2002, in J. S. Mulchaey & J. Stocke (eds.), *Extragalactic Gas at Low Redshift*, *ASP-CS*, 254, 267
- Bland-Hawthorn, J., Sutherland, R., Agertz, O., & Moore, B. 2007, *ApJ*, 670, L109
- Bregman, J. N. 2007, *ARAA*, 45, 221
- Brüns, C., Kerp, J., Staveley-Smith, L., *et al.* 2005, *A&A*, 432, 45
- Chevalier, R. A. & Raymond, J. C. 1978, *ApJ*, 225, L27
- Connors, T. W., Kawata, D., & Gibson, B. K. 2006, *MNRAS*, 371, 108
- Ferrara, A. & Field, G. B. 1994, *ApJ*, 423, 665
- Flynn, C., Holmberg, J., Portinari, L., Fuchs, B., & Jahreiß, H. 2006, *MNRAS*, 372, 1149
- Gibson, B. K., Giroux, M. L., Penton, S. V., Putman, M. E., Stocke, J. T., & Shull, J. M. 2000, *AJ*, 120, 1830
- Kallivayalil, N., van der Marel, R. P., & Alcock, C. 2006, *ApJ*, 652, 1213
- Lockman, F. J., Benjamin, R. A., Heroux, A. J., & Langston, G. I. 2008, *ApJ*, 679, L21
- Madsen, G. J., Haffner, L. M., & Reynolds, R. J. 2002, in A. R. Taylor, T. L. Landecker, & A. G. Willis (eds.), *Seeing Through the Dust. The Detection of H1 and the Exploration of the ISM in Galaxies*, *ASP-CS*, 276, 96
- Maloney, P. R. & Bland-Hawthorn, J. 1999, *ApJ*, 522, L81
- Maloney, P. 1993, *ApJ*, 414, 41
- Mastropietro, C., Moore, B., Mayer, L., Wadsley, J., & Stadel, J. 2005, *MNRAS*, 363, 509
- Miyamoto, M. & Nagai, R. 1975, *PASJ*, 27, 533
- Moore, B. & Davis, M. 1994, *ApJ*, 270, 209
- Peek, J. E. G., Putman, M. E., & Sommer-Larsen, J. 2008, *ApJ*, 674, 227
- Piatek, S., Pryor, C., & Olszewski, E. W. 2008, *AJ*, 135, 1024
- Putman, M. E., Bland-Hawthorn, J., Veilleux, S., Gibson, B. K., Freeman, K. C., & Maloney, P. R. 2003, *ApJ*, 597, 948
- Quilis, V. & Moore, B. 2001, *ApJ*, 555, L95
- Rosen, A. & Smith, M. D. 2004, *MNRAS*, 347, 1097
- Sembach, K. R., Howk, J. C., Savage, B. D., Shull, J. M., & Oegerle, W. R. 2001, *ApJ*, 561, 573
- Sembach, K. R., Wakker, B. P., Savage, B. D., *et al.* 2003, *ApJS*, 146, 165
- Slavin, J. D., Shull, J. M., & Begelman, M. C. 1993, *ApJ*, 407, 83
- Smith, M. C., Ruchti, G. R., Helmi, A., *et al.* 2007, *MNRAS*, 379, 755
- Wakker, B. P., York, D. G., Howk, J. C., *et al.* 2007, *ApJ*, 207, 670, L113
- Weiner, B. J., Vogel, S. N., & Williams, T. B. 2002, in J. S. Mulchaey & J. Stocke (eds.), *Extragalactic Gas at Low Redshift*, *ASP-CS*, 254, 256
- Westmeier, T. & Koribalski, B. S. 2008, *MNRAS*, 388, L29
- Wilkinson, M. I. & Evans, N. W. 1999, *MNRAS*, 310, 645
- Williams, J. P. & McKee, C. F. 1997, *ApJ*, 476, 166
- Wolfire, M. G., McKee, C. F., Hollenbach, D., & Tielens, A. G. G. M. 1995, *ApJ*, 453, 673